

Morphological and Electrical properties of transition metal ion substituted Calcium hexagonal nano ferrites synthesized by Sol gel auto-combustion method.

B.S.Satone¹, K.G.Rewatkar²,

¹Department of Physics, S.H.J.C., Nagpur

²Department of Physics, Dr. Ambedkar college, Nagpur.

Abstract—In the present research module the samples with chemical composition $\text{CaMeFe}_{11}\text{O}_{19}$ (where Me =La, Cr and Al) have been chosen for their studies on structural and electric properties. Above samples were successfully synthesized by sol gel auto combustion method in which the urea was used as a fuel. The XRD pattern revealed the formation of mono phase hexagonal ferrites with space group $P6_3/mmc$ (No.194). The SEM and TEM results confirmed that the sample exhibit relatively well defined hexagonal like grains with average particle size in the range 52 nm to 38nm. The values of the lattice parameters supports this conformation.

Electrical conductivity is measured by two probe method using Wyne Kerr 6500B model. The variation of DC conductivity in terms of $(\log \sigma)$ with reciprocal of temperature and was studied. It is explained on the basis of Verwey model. The variation of dielectric constant with \log frequency and loss tangent with temperature for all samples were analyzed on the basis of Maxwell Wagner and Koop's model.

Keywords—M type ferrite, Sol-gel Auto-combustion, XRD, TEM, Dielectric constant, Activation energy etc.

I. INTRODUCTION

Ferrites continued to attract attention of researchers over the years due to their broad category of applications over wide frequency range, low cost and high performance [1]. In 1952, a new class of ferrites so-called hexagonal ferrites with formula $\text{M}(\text{Fe}_{12}\text{O}_{19})$ having permanent magnetic properties were discovered, where M is usually barium (Ba), strontium (Sr), calcium (Ca) or lead (Pb) [2]. Due to large “built in” biasing field, these materials have good prospects for application in microwave devices, memory core, perpendicular magnetic recording and permanent magnets.[3-5]. The Calcium ferrite having general formula $\text{CaFe}_{12}\text{O}_{19}$ is one of the most important hard magnetic materials, widely used for above applications [6-8]. A number of researchers have reported microwave attenuation in M type hexaferrites by increasing magnetic losses. Alternatively dielectric losses can also accompany attenuation in ferrites. [9].

The M type Polycrystalline nanoferrite are very good dielectric materials and very useful for microwave applications. The study of dielectric properties offers valuable information about the behavior of localized electric charge carriers and can explain the mechanism of electrical conduction and dielectric polarization. The substitution of small amount of magnetic or non-magnetic ions brings an important modification in the structural and transport properties of these materials [10].These applications need significant magnetic and electrical specifications and in this view, several attempts have been made to modify the properties of hexagonal ferrites using different processing route including external doping [11-113]. Recently the research on ferrite have been shifted towards developing ferrites at nanometric scale due to its unique mechanical, electrical, optical and magnetic properties. The unique property of nanostructure materials are due to changed electronic structure closed to that of isolated atom or molecule [14].

To prepare nanosized ferrite particles several methods were investigated, all methods produce same microstructure. In current research module we used the sol gel auto combustion method to

synthesis the calcium substituted hexaferrite powders as this method is simple, safe, rapid and main advantages of this method is high homogeneity, high purity and producing ultrafine powders [15]. The aim of the present work is to synthesize substituted nanosized CaM hexaferrites by sol gel auto combustion technique and reports experimental results for their structure, dielectric behaviour and possible uses at different frequencies.

II. EXPERIMENTAL

The samples of $\text{CaMeFe}_{11}\text{O}_{19}$ (where Me = La, Cr and Al) were synthesized by sol gel auto-combustion method. The reactive nitrates such as $\text{Ca}(\text{NO}_3)_2 \cdot 4\text{H}_2\text{O}$, $\text{Fe}(\text{NO}_3)_3 \cdot 9\text{H}_2\text{O}$, $\text{La}(\text{NO}_3)_3 \cdot 9\text{H}_2\text{O}$ / $\text{Cr}(\text{NO}_3)_3 \cdot 9\text{H}_2\text{O}$ / $\text{Al}(\text{NO}_3)_3 \cdot 9\text{H}_2\text{O}$ were taken in stoichiometric proportions, dissolved into distilled water and heated at the temperature of 80°C for about 3 hr with urea used as fuel, which gives requisite energy to initiate exothermic reaction. The gel formed were fired in digitally controlled microwave oven, yielding powder (ash), which were followed by grinding for about 5 hours in pestal mortar to get ultra-fine homogeneous powder of samples. The resulting powder then heated in electric furnace up to 800°C for about 8 h by increasing the temperature slowly ($100^\circ\text{C}/\text{hr}$) and then cooled at the same rate. Finally the powder samples of all the specimens were then subjected to the structural characterization and for electrical measurements crack free pellets of corresponding samples were used.

The phase structure of hexaferrite powders were investigated by (Philips diffractometer PW 3710) X ray diffraction $\text{Cu-K}\alpha$ radiation ($\lambda = 1.54060\text{\AA}$). The Phase identification was executed using a X powder software and X-ray diffractograms were also plotted with X-Powder software. The structure morphology was identified using SEM instrument Cameca SU – SEM Probe and the TEM studies of prepared samples were done by using TEM Model Philips CM – 200. The DC electrical properties such as conductivity, resistivity, activation energy and transition temperature of prepared ferrite samples were studied in the temperature range 300K to 700K by using four probe method (Wyne Kerr 6500B model).

III. RESULTS & DISCUSSION

The diffraction peaks in XRD patterns (Fig.1) of the investigated ferrite samples synthesized by sol gel auto-combustion technique corresponds to M-type calcium ferrite structure. Absence of secondary peaks in XRD pattern confirms the formation of purely crystallized single phase [16] hexagonal M-structure with space group (SG: $\text{P6}_3/\text{mmc}$) (No.194), which confirms that phase belongs to Magnetoplumbite, indicating that the crystal structures were single phase hexagonal magnetoplumbite after substitution with La^{3+} , Cr^{3+} , Al^{3+} ions respectively. The recorded lattice parameters values lie within the range ($a = 5.8\text{--}5.9\text{ \AA}$ and $c = 22\text{--}23\text{ \AA}$) of pure magnetoplumbite phase of hexaferrites which also strengthen the results. Moreover, the intensity of the peaks becomes stronger and narrower, indicating a better structural quality of materials [17]. The average particle size D of samples were calculated from Scherrer formula [18] reveals size in nanometer scale. The particle size of ferrites were in the range 38 – 56 nm, which was also confirmed by SEM and TEM studies, (fig. 2) and (fig.3).

The compositional dependence of the lattice parameters, bulk density (d), X-ray density (d_x), porosity (P) and average particle size of all the samples are listed in Table 1. The variations of lattice parameters (a , c) shown in Table 1. can be attributed to substituted cations as the ratio of c/a has remained fairly constant. The lattice parameter ' a ' remains almost constant and ' c ' decrease, It can also be explained on the basis of ionic radii, as Fe^{3+} ions were replaced by Me ions (where Me = La^{3+} , Al^{3+} , Cr^{3+}) of lower radius at $2b$ or $4f_2$ octahedral site associates to enlargement in the value of $2b\text{--O}^{2-}\text{--}4f_2$ bond angle, due to this, decrease in lattice constants were observed in hexaferrites [19]. Similar nature was observed for replacement of Sr^{2+} ion by La^{3+} ion by D Selfert et.al. [20] and for Mn–Zn substituted Ca-hexaferrite by C.L. Khobragade [21] on the basis of having lower radius which decreases the distance between stacking layer.

It is evident that for the content Al^{3+} the lattice parameters are smaller as compared to the contents Cr^{3+} and La^{3+} respectively. This is due to relatively small ionic radius of Al^{3+} (0.53 Å) compared to that of Cr^{3+} (0.62 Å) and La^{3+} (1.03 Å) respectively. Analogous behavior was reported for Me substituted calcium ferrite by Prakash et al. (where Me = Al, Cr and Co) [22] and Co-Al substituted calcium ferrite by Rewatkar et al. [23]. Due to relatively small lattice constant and particle size interaction and solubility between Fe^{3+} ion and Al^{3+} ion is higher than other trivalent ions in the investigated compounds.

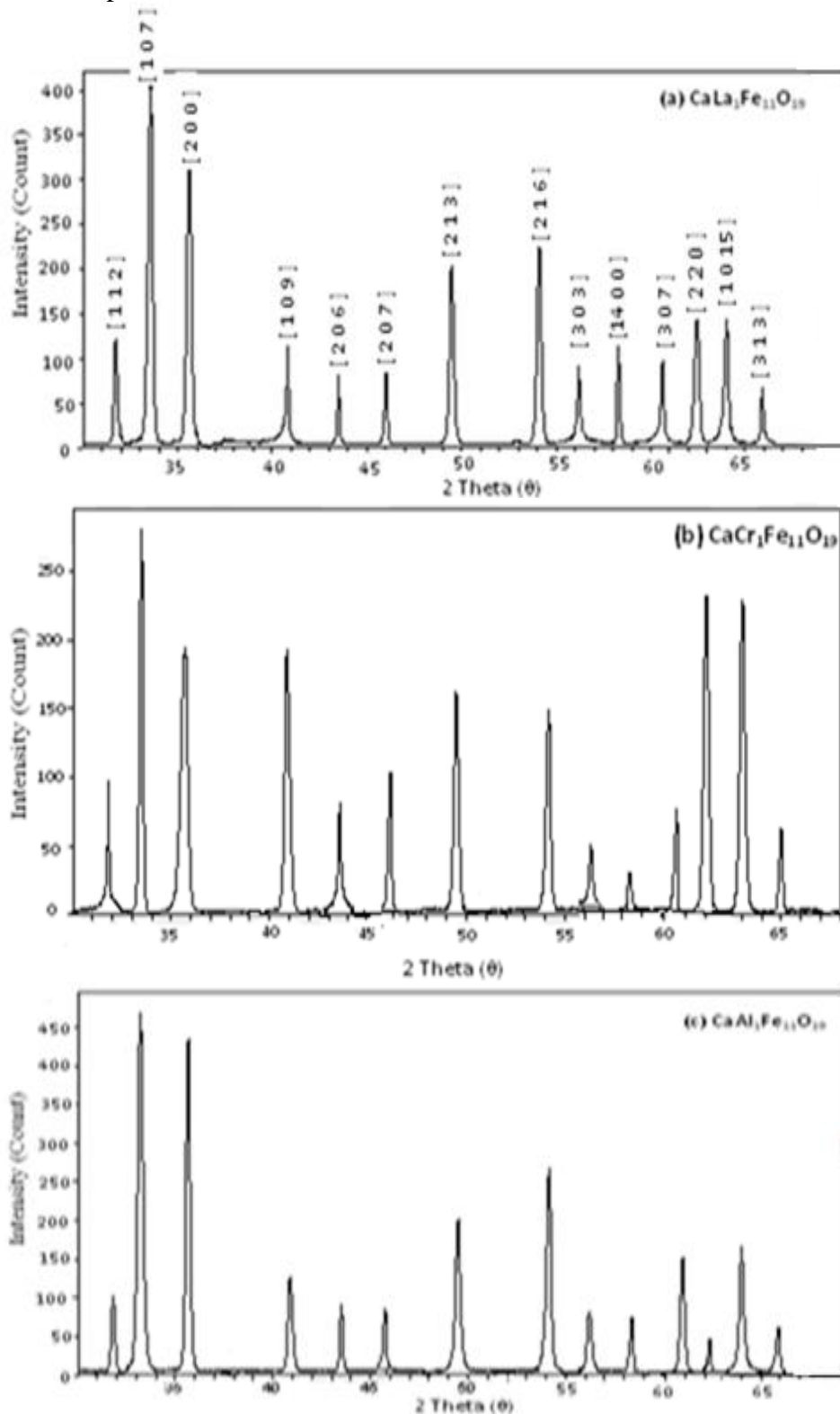


Fig. (1): XRD Pattern of synthesized Ca Substituted Hexaferrite

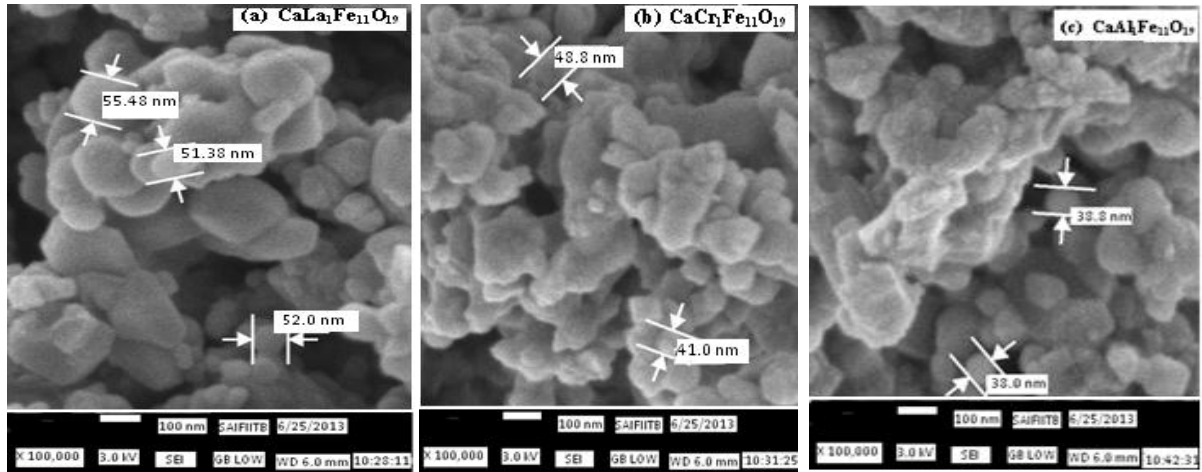


Fig. (2): SEM Micrographs of Synthesized compounds

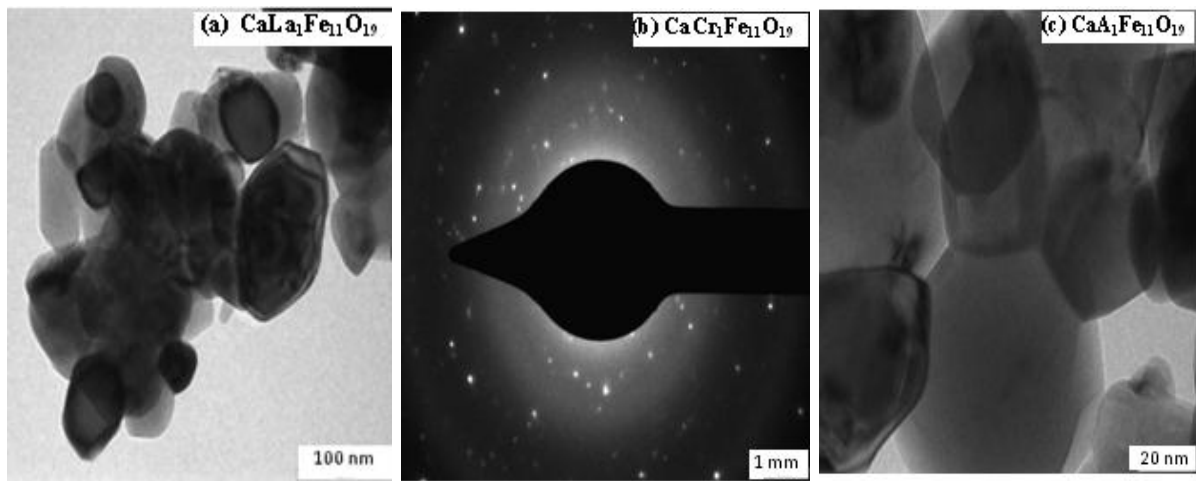


Fig. (3): TEM Micrographs of Synthesized compounds

Table 1: Structural data

S.No.	sample	Lattice parameters		Axial ratio c/a	Cell vol. (Å) ³	Bulk density, (d) (gm/cm ³)	X-ray density, d _x (gm/cm ³)	Porosity (p) %	Particle size (D) nm
		a (Å)	c (Å)						
1	CaLa ₁ Fe ₁₁ O ₁₉	5.8201	22.1164	3.80	647.55	2.0429	5.6237	63	56
2	CaCr ₁ Fe ₁₁ O ₁₉	5.8179	22.1079	3.80	647.15	2.6201	5.0505	48	43
3	CaAl ₁ Fe ₁₁ O ₁₉	5.8112	22.0826	3.80	646.67	3.3529	5.1881	35	38

The variation in the densities shows linear behavior that is the X-ray density (theoretical density d_x) is higher than actual density (experimental density d). During firing oxygen ions diffuses through the materials creating unavoidable pores, which is one of the factor deciding the densification of the samples [24]. The variation in porosity attributes to function of lattice parameters; it is reported that if densification increases, the volume of unit cell and lattice constant ultimately decrease and vice-versa [25] this is in good agreement with our results.

Sample	Activation Energy E_g in eV		Resistivity at Room temperature $\Omega\text{-cm}$	Conductivity at room temperature $(\Omega\text{-cm})^{-1}$	Transition Temperature (K)
	Paramagnetic	Ferrimagnetic			
$\text{CaLa}_1\text{Fe}_{11}\text{O}_{19}$	0.59	0.28	1.76×10^7	5.69×10^{-8}	565
$\text{CaCr}_1\text{Fe}_{11}\text{O}_{19}$	0.53	0.31	3.20×10^7	3.12×10^{-8}	530
$\text{CaAl}_1\text{Fe}_{11}\text{O}_{19}$	0.35	0.17	2.65×10^7	3.77×10^{-8}	525

Table 2: Electrical resistivity and Transition temperature

The values of electrical parameters such as conductivity, resistivity, activation energy and transition temperature of prepared ferrite samples were enumerated in table 2. It is evident that the conductivity decreases with doping of Me^{+3} ions for Fe^{+3} ions (where $\text{Me} = \text{La}, \text{Al}, \text{Cr}$). Variation of DC electrical conductivity in terms of $\log \sigma$ with inverse absolute temperature of all samples are shown in figure (4). From these plots it is seen that, the resistivity decreases with increasing temperature for all samples, showing negative temperature coefficient of resistivity. This is normal semiconductor behavior. This is like the results reported for Cr^{3+} substituted ferrite by S.A. Masti [26]. The values of $\log \sigma$ decreases almost linearly with increasing reciprocal temperature up to certain temperature (T_i), where a change in slope (kink) occurs in the plot in the neighborhood of its magnetic transition temperature (T_i). This reveals that the kink observed in the samples undertaken in this research module can be attributed to the magnetic order phase transition from ferri to paramagnetic state. Comparatively close results were reported for Ba-Mg hexaferrite powder by Chetna C et al. [27] and for Lithium hexaferrites powder by G. Arvind et al. [28]. This may also be possible due to formation of other secondary phases and decrease in porosity of the samples. The decrease in porosity causes the close packing between the grains. This close packing could have exerted retarding force on charge carriers which may lead to the difficulty for the conduction of the free electrons from grain to grain as suggested by Abbs et al. [29]. From the plot of $\log \sigma$ vs. $10^3/T$ the activation energy was calculated in the neighborhood of magnetic transition temperature. It was observed that the activation energy in paramagnetic region is more than that in the ferrimagnetic region. It can be interpreted as there is magnetic disorder state in paramagnetic region as compared to ferrimagnetic region [30]. The increase in activation energy may be attributed to the creation of more cations and development of oxygen vacancies which might have become more productive due to rise in temperature. It is concluded that concentration of oxygen vacancies is an important factor in sintering process as well as DC electrical resistivity as suggested by S. Kumar et al. [31]. The electrical conduction in such ferrites can also be explained by Verwey hopping mechanism of electron [32]. Accordingly, electronic conduction in ferrites at room temperature occurs due to the impurities whereas at high temperature it is due to polaron hopping. According to

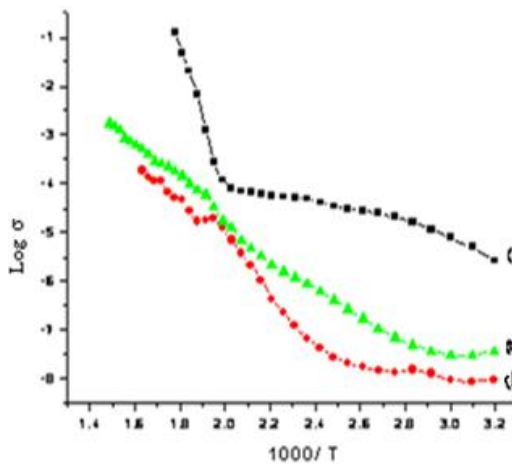


Fig. (4): Temperature dependence of conductivity of samples

(a) $\text{CaLa}_1\text{Fe}_{11}\text{O}_{19}$, (b) $\text{CaCr}_1\text{Fe}_{11}\text{O}_{19}$ and (c) $\text{CaAl}_1\text{Fe}_{11}\text{O}_{19}$ at fixed frequency

more productive due to rise in temperature. It is concluded that concentration of oxygen vacancies is an important factor in sintering process as well as DC electrical resistivity as suggested by S. Kumar et al. [31]. The electrical conduction in such ferrites can also be explained by Verwey hopping mechanism of electron [32]. Accordingly, electronic conduction in ferrites at room temperature occurs due to the impurities whereas at high temperature it is due to polaron hopping. According to

Verwey, hopping mechanism in electronic conduction in ferrites is mainly due to electron hopping exchange between ion ($\text{Fe}^{+3} + \bar{e} \rightarrow \text{Fe}^{+2}$) of same element, present in more than one valence state, distributed randomly over crystallographically equivalent lattice sites [33].

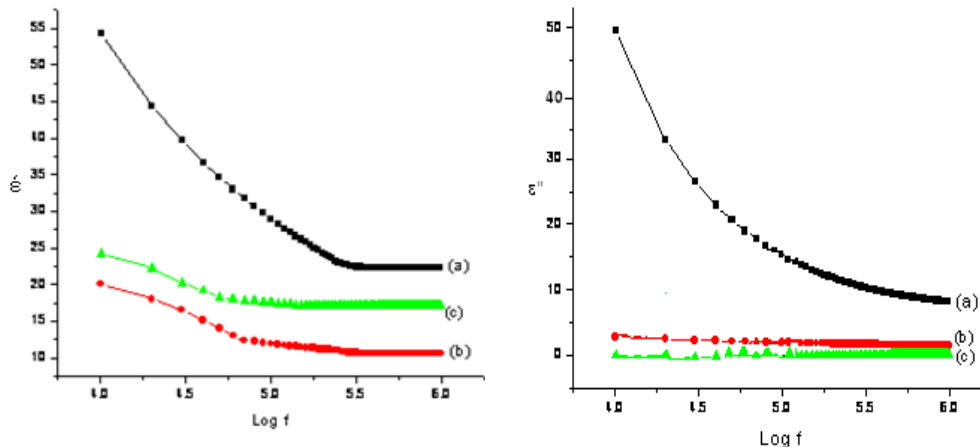


Fig. (5): variation of of $\log f$ against (i) dielectric constant (ϵ') and (ii) dielectric loss (ϵ'') for samples (a) $\text{CaLa}_1\text{Fe}_{11}\text{O}_{19}$, (b) $\text{CaCr}_1\text{Fe}_{11}\text{O}_{19}$ and (c) $\text{CaCr}_1\text{Fe}_{11}\text{O}_{19}$ respectively.

The effect of frequency on dielectric behavior offers much valuable information about the localized charge carrier which in turn helps to elucidate the mechanisms responsible for charge transport phenomena and dielectric behaviour. The variation of real and imaginary parts of dielectric constant (ϵ') and dielectric loss (ϵ'') for all samples sintered at 800°C as a function of log frequency from 100 Hz to 1 MHz at room temperature are shown in figure (5). It is observed that at low frequencies ϵ' and ϵ'' has high values, decreases with increase in frequency, showing more dispersion in low frequency region (100Hz to 1kHz), then decreases slowly in high frequency region (1kHz to 1MHz) and finally it remains almost independent of applied external field at high frequency region and becomes constant. All the samples reveal dispersion due to Maxwell-Wagner type interfacial polarization (1913) in agreement with Koop's phenomenological theory (1951) [34,35]. According to these models, the dielectric material with a heterogeneous structure can be imagined as a structure consists of well conducting grains separated by highly resistive thin layers (grain boundaries). In this case, the applied voltage on the sample drops mainly across the grain boundaries and space charge polarization is built up at the grain boundaries [36]. Due to this fact the dielectric material exhibit induced electric moment under the influence of external electric field.

The higher values of dielectric constant observed at low frequencies are explained on the basis of space charge polarization due to inhomogeneous dielectric structure and resistivity of the samples [37]. The inhomogeneities in the present system are impurity, porosity and grain structure [38]. The decrease in dielectric constant with increasing frequency is attributed to the electron exchange between Fe^{2+} and Fe^{3+} ions cannot follow the change of the external applied field beyond certain frequency. This decreases the probability of electrons reaching the grain boundaries and as a result polarization decreases [39]. At higher frequency, the polarization of the induced moment could not synchronize with the frequency of applying electric field. So dielectric attains a constant value above certain high frequencies [40]. Such type of behaviour in rare earth substituted Ca hexaferrites is a common ferrimagnetic behaviour and also been observed by other investigators [41-43]. It is evident from Table 2 that the activation energy of paramagnetic region (E_p) is greater than that of ferrimagnetic region (E_f). Our results on electrical properties are in good agreement with the other reported nano-size spinel ferrite systems [44].

Loss tangent or loss factor $\tan \delta$ represents the energy dissipation in the dielectric system. It is considered to be caused by domain wall resonance. At higher frequency the losses are found to be low since domain wall motion is inhibited and magnetization is forced to change rotation Alimuddin A. M. M Farea et al. [45]. Fig. (6) shows the variation of $\tan \delta$ with temperature for all samples. It is

observed that in general, $\tan\delta$ has small values and indicates a peak at different temperature for the samples of different doping materials. For the samples $\text{CaLa}_1\text{Fe}_{11}\text{O}_{19}$, $\text{CaCr}_1\text{Fe}_{11}\text{O}_{19}$, $\text{CaAl}_1\text{Fe}_{11}\text{O}_{19}$, peak appears at around 570K, 550K and 530K respectively. The dielectric loss tangent ($\tan\delta$) can be explained on the basis of polarization effect.

The dielectric polarization increases with increase in temperature which causes the increase in dielectric loss tangent ($\tan\delta$), there is resemblance in behaviour were reported by other investigators [46,47]. The appearance of a maximum in $\tan\delta$ could be explained according to Koops's model [48] in which the solid is assumed to be composed of grains and grain boundaries. Each one has different parameters, where the grains have low resistivity and large thickness while the grain boundaries have high resistivity and small thickness. Moreover, it was assumed that [49] each of the grains and grain boundaries has its characteristic peak. Thus the observed peak in $\tan\delta$ may be attributed to the contribution from the grain boundaries, where the impurities reside, which take part in the conduction at low temperatures. The role of the grains may appear at higher temperatures [50].

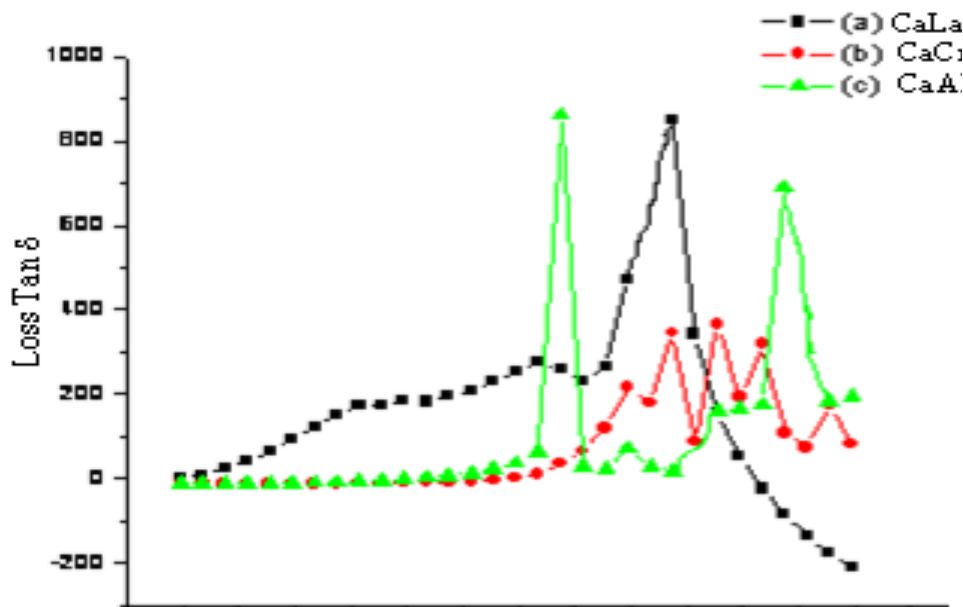


Fig. (6): variation Temperature (T) against D-factor (loss - $\tan\delta$) for all prepared samples.

IV. CONCLUSION

The samples of Lanthanum, Chromium and Aluminium doped calcium hexaferrites were successfully synthesized by the microwave induced sol-gel auto combustion method. The XRD analysis of all samples confirms the formation of mono phase M-type hexagonal structure. The average size of the particles deduced from XRD peak broadening have been observed to lie in the range 52 nm to 32 nm. The values of the lattice parameters, SEM and TEM study supports this conformation. The space group of synthesized samples is found to be $P6_3/mmc$. (No. 194).

The dc electrical conductivity reveals that prepared samples exhibit semiconducting nature. From variation of $\log\sigma$ and reciprocal of temperature, the transit temperature is found to be 565K, 530K and 525K for samples respectively. The activation energy in paramagnetic region is more than that in the ferrimagnetic region for all the samples. This can be attributed to the magnetic phase transition, which is the transition from order to disorder. Disorder provides resistance to the conduction.

The dielectric behaviour shows strong frequency as well as composition dependence. The relatively high values of the dielectric constant at low frequency and rapid decrease in it with increasing frequencies and reaching a constant value at higher frequency can be explained fairly on the basis of space charge polarization (Koop's Model). The dielectric constant (ϵ'), and dielectric loss factor (ϵ'') both shows same nature with increase in frequency. The dielectric loss tangent ($\tan\delta$) has small values and peak is obtained at particular temperature which could be explained according to Koops's model.

Higher value of DC resistivity and low dielectric losses suggest that the prepared materials have great potential for microwave and high frequency applications as well as they are promising material for use in transformers cores and in motors that work at relatively low frequency.

REFERENCES

- [1] J. Wang, P. F., Chong., S. C. Ng and L. M. Gan, "Microemulsion processing of manganese zinc ferrites" *Materials Letters.*, Issue2-3, vol. 30, pp 217-221, Feb. 1997.
- [2] R. Dosoudil, M. Usakova, J. Franek, J. slama and V. Olah," RF Electromagnetic wave absorbing properties of ferrite polymer composite materials", *J. Magn. Magn. Mater.* Vol.304, pp755-757, 2006.
- [3] B. Lax, and K.J. Button, "Microwave Ferrites and Ferrimagnetics", McGraw Hill Book Co., (1962).
- [4] I. Wane, A Bessaudou, F Cosset, A Célérier, C Girault, J.L Decossas, J.C Vareille, " Thick barium hexaferrites (Ba-M) films prepared by electron beam evaporaton for microwave applications", *J. Magn. Magn. Mat.*, Issue (1-2), Vol. 211, pp 309-313, Mar. 2000.
- [5] S. B. Narang and I.S. Hudiarra. "Microwave dielectric properties of M-Type barium, calcium and strontium hexaferrite substituted with Co and Ti" *Journal of Ceramic Processing Research.*, Issue 2, Vol. 7, pp. 113-116, (2006),
- [6] A. Franco, and F.C. de Silva, "High temperature magnetic properties of cobalt ferrite nanoparticles", *Applied. Physics. Letters*, Issue 17, Vol.96, (id 172505), Apr. 2010.
- [7] R. He, X. You, J. Shao, F. Gao, B. Pan, and D. Cui, "Core/Shell fluorescent magnetic silica-coated composite nanoparticles for bioconjugation, *IOP Publishing Ltd, Nanotechnology*, Issue31, Vol. 18, 2007.
- [8] M. Veverka, P. Veverka, O. Kaman, A. Lančok, K. Závěta, E. Pollert, K. Knížek, J. Boháček, M. Beneš, P. Kašpar, E. Duguet, and S. Vasseur, "Magnetic heating by cobalt ferrite nanoparticles", *IOP Publishing Ltd, Nanotechnology*, Issue 34, Vol. 18, July 2007.
- [9] C. Singha, S. B. Narang, I. S. Hudiarra, K. C. James, R. K. Sudheendran., "Microwave and electrical properties of Co-Zr substituted Ba-Sr ferrite", *Journal of Ceramic Processing Research*", Issue 6, Vol.11, pp 692-697, 2010.
- [10] A. T. Pathan, A. M. Shaikh, Dielectric properties of Co-substituted LI-Ni-Zn Nanostructured ferrites prepared through chemical route, "Int. J. Computer Applications", Issue21, Vol. 45, pp 24-28, May 2012.
- [11] B. S. Satone, A. S. Kakde, M. J. Gothe, K. G. Rewatkar, P. S. Sawadh, "Morphological and dielectric behavior of Cr substituted nanosized calcium hexaferrites by sol gel autocombustion technique", *Int. J. Res. in Biosciences, Agriculture and Tech.* ", Issue 2, Vol.1, pp 949 – 955, Jan. 2014.
- [12] M.M. Costa, G.F.M. Pires Junior, A.S.B. Sombra., "Dielectric and impedance properties' studies of the of lead doped (PbO)-Co₂Y type hexaferrite (Ba₂Co₂Fe₁₂O₂₂ (Co₂Y))" *Int. J. Mat. Chem. And Phy.*, Issue 1, Vol.123, pp35–39, Nov.2010.
- [13] R. M .Sanshetti, Vahiremath, V.M.Jali., "Combustion synthesis and structural characterization of Li-Ti mixed nanoferrites" *Bull. Matter. Sci*, Issue 5, Vol 34, pp 1027-1031, Aug 2011.
- [14] A. M. Bhavikatti, S. Kulkarni, A. Lagashetty, Characterization and electromagnetic studies of nano-sized barium ferrite", *Int. J. of Eng. Sci. and Tech.* (ISSN: 0975-5462), Issue 11, Vol. 2, pp 6532-6539, 2010.
- [15] S. R.Gavali, K.G.Rewatkar, and V. M.Nanoti, Structural and Electrical properties of M-type Nanocrystalline Aluminium substituted Calcium Hexaferrites", *Adv. in Appl. Sc. Res.* (ISSN: 0976-8610), Issue 5, vol.3, pp-2672-2678, 2012.
- [16] R. H. Kadam, A. Karim, A. B Kadam, A.S. Gaikwad ,S.E. Shirsath, Influence of Cr³⁺ substitution on the electrical and magnetic properties of Ni_{0.4}Cu_{0.4}Zn_{0.2}Fe₂O₄ nanoparticles", *Int. nanoletters*, Issue28, Vol.2, pp2:28, Oct. 2012.
- [17] S. N. Sable, K. G. Rewatkar, V.M. Nanoti, "Structural and Magnetic Behavioral Improvisation of Nanocalcium Hexaferrites", *Materials Science and Engineering*, Issue 1-3, Vol. 168, pp 156-160, Apr 2010.
- [18] S. Khorrami, F. Gharib, G. Mahmoudzadeh, S. Sadat SepehrS. Sadat Madani, N. Naderfar, S. Manie "Synthesis and characterization of nanocrystalline spinel Zinc ferrite prepared by sol-gel auto-combustion technique", *Int. J. Nano. Dim.* (ISSN: 2008-8868) ,Issue3, Vol 1, pp 221-224, Winter 2011.
- [19] R. Mahadule, P. Arjunwadkar , M. Mahabole., "Structural, Dielectric and Magnetic Properties of La-M Hexaferrite" *Int. J. of Scientific & Eng. Research*, (ISSN 2229-5518), Issue 7, Volume 4, pp 2486-2496, July-2013.

- [20] D. Seifert, J.T. Opfer, F. Langenhorst, J.-M. Le Breton, H. Chiron, L. Lechevallier, "Synthesis and magnetic properties of La-substituted M-type Sr hexaferrites", *J. Magn. Magn. Mat.*, Issue 24, Vol.321, pp 4045-4051, Dec 2009.
- [21] C. L. Khobragade, "Structural, mechanical, electrical & magnetic properties of," *Journal Materials & Metallurgical Engg*, Issue 3, vol. 1, pp. 1-9, 2011.
- [22] C. S. Prakash and D. K. Kulkarni "Variational effect in substituted calcium hexaferrites", *International Journal of Knowledge Engineering* (ISSN: 0976-5816 & E-ISSN: 0976-5824), Issue 1, Volume 3, pp.-79-80, Mar. 2012.
- [23] K. G. Rewatkar, N. M. Patil, S. R. Gawali, "Synthesis and magnetic study of Co-Al substituted calcium hexaferrites", *Bull. Mater. Sci*, Issue 6, Vol. 28, pp 585-587, Oct 2005.
- [24] A. Deshpande, S. N. Sable, V. M. Nanoti, K. G. Rewatkar, "Studies of structural and electrical properties of ZrCo substituted Ca hexa-ferrites" *Int. J. Kno. Eng.* (ISSN: 0976-5816 & E-ISSN: 0976-5824), Issue 1, Vol. 3, pp 140-142, 2012.
- [25] K. G. Rewatkar, N. M. Patil, S. Jaykumar, D. S. Bhowmick, M. N. Giriya., "Synthesis and the magnetic characterization of iridium-cobalt substituted calcium hexaferrites" *J. magn. Magn. Mat.*, Issue 1, Vol. 316, pp 19-22, Sep. 2007.
- [26] S. A. Masti, "Crystallographic and electrical resistivity study of Cr³⁺ substituted Mg-Cd ferrites for low loss power devices", *Int. J. of Advances in Engineering & Technology*, (ISSN:22311963), Issue 6, Vol. 6, pp. 2433-2438, Jan. 2014.
- [27] C.C. Chauhan, R. B. Jotania, K. R. Jotania, "Conductivity and dielectric properties of M-type barium magnesium hexaferrite powder", *Int.J.of Adv. Eng. Res. and Studies* (E-ISSN2249-8974), Issue 4, Vol. 1, pp 25-27, Jul-Sep., 2012.
- [28] G. Aravind and D. Ravinder, "Synthesis, Structural & Dielectrical Properties of Citrate-Gel Prepared Lithium Nano Ferrites" *Int. J. of Eng. Research and Applications*, (ISSN : 2248-9622), Issue 6, Vol.3, pp.1033-1039, Nov-Dec 2013.
- [29] S. M. Abbas, R. Chatterjee, A. K. Dixit, A. V. R. Kumar, & T. C. Goel., "Electromagnetic and microwave absorption properties of (Co²⁺-Si⁴⁺) substituted barium hexaferrites and its polymer composite". *J. of App. Phy.*, (ISSN 0021-8979), Issue 7. Vol.101, pp. 074105-6, Apr. 2007.
- [30] A. Deshpande, S. N. Sable, V. M. Nanoti, K. G. Rewatkar., "Studies of structural and electrical properties of ZrCo substituted Ca hexa-ferrites", *International Journal of Knowledge Engineering*, (ISSN: 0976-5816 & E-ISSN: 0976-5824), Issue 1, Volume 3, pp.-140-142, Mar. 2012,
- [31] S. Kumar, G. Kumar and M. Singh, "Effect of temperature on structural and electrical properties of Mn_{0.6}Zn_{0.2}La_{0.2}Fe₂O₄ Nanoferrite", *J Integr Sci Technol*, Issue 1, Vol.3, pp1-5, 2015.
- [32] E. J. W. Verwey, J. H. De Boer. "Cation arrangement in a few oxides with crystal structures of the spinel type. *Rec. Trans. Chim. Des Pays-Bas*", Vol.55, PP 531-540, 1936.
- [33] R. Mahadule R, P. Arjunwadkar, M. Mahabole, "Frequency and Compositional Variation of Dielectric Parameters for La substituted M-Hexaferrite", *IOSR Journal of Engineering (IOSRJEN)* e-ISSN: 2250-3021, p-ISSN: 2278-8719, Issue 11, Vol. 2, PP 12-16, Nov. 2012.
- [34] M. Snaikh, S. S. Bellard, B. K. Chougule "Temperature and frequency dependent dielectric properties of Zn substituted Li-Mg ferrites", *J. Magn. Magn. Mater.*, Vol. 195, pp. 384-390, 1999.
- [35] M.A. Ahamad, J. Elhiti, "Electrical and dielectric properties of Zn_{0.8}Co_{0.2}Fe₂O₄", *Physique*, Issue 3, Vol.5, pp.775, 1995.
- [36] S. D. More, C. M. Kale, A. B. Shinde, K. M. Jadhav, "Role of Cr³⁺ Substitution on Electrical and Dielectric Behavior of Cu-ferrite Nanoparticles" *International Journal of Engineering and Advanced Technology (IJEAT)* ISSN: 2249 - 8958, Issue-2, Volume-3, pp 177-180, December 2013.
- [37] K. W. Wagner, "Zur Theorie der Unvollkommenen Dielektrika. *Ann Physik Bd*", 40 (1913) 817.
- [38] J. C. Maxwell "Electricity and Magnetism", Vol. 1, Section 828, Oxford University press, New York, 1973.
- [39] E. Chaturvedi, K. G. Rewatkar, V. M. Nanoti, "Improvement in morphological and electromagnetic behaviour of Hard ferrite permanent magnets based on Ni-Ir substitution" *Int. J. of Modern Trends in Eng. and Research (IJMTER)*, (e-ISSN: 2349-9745, p-ISSN: 2393-8161), Issue 01, 707-710, Volume 02, pp Jan. 2015.
- [40] A. Katoch, T. Singh, B.S Sandhuc "Influence of doping of rare earth ion (Re=La) on structural, electrical and dielectric properties of SrM-hexaferrite" *International Journal of Research in Advent Technology*, (E-ISSN: 2321-9637), Issue 5, Volume 1, pp 456-465, Dec. 2013.
- [41] A. Katoch, A. Singh, T. Singh., "Electrical And Dielectric Properties of M-Type Strontium Hexaferrites Doped With Gd-Rare Earth Ions", *International Journal of Engineering Research & Technology (IJERT)* (ISSN: 2278-0181), Issue 3, Vol. 2, pp 1-6, Mar. 2013.
- [42] V. V. Awati, D. H. Bobade, Mrs S. D. Kulkarni, S.M. Rathod, "Structural, Dielectric and Magnetic Behavior of Cu²⁺ Substituted Ni-Zn Ferrite by Auto-combustion Technique", *International Journal of Engineering Research and Applications (IJERA)* ISSN: 2248-9622, Issue 6, Vol. 2, pp.482-489, November- December 2012,
- [43] Ch. Mamtha, M. Krsnaiah, C. S. Prakash, K. G. Rewatkar, "Structural and electrical properties of Al substituted Nano Ca. ferrites" *Int. con. on Adv. in Man. and Mat. Eng.*, (AMME 2014), *Procedia Materials science*, Vol. 5, pp780 - 786, 2014.

- [44] P. R. Moharkar, S. R. Gawali, K. G. Rewatkar, V. M. Nanoti, "Improvisation of Structural, Electrical and Magnetic Properties of Nanocrystalline Ca_{2-y} Hexaferrite on Al-Substitution" Proc. Int. J. of Com. Appl. (IJCA), pp 1-5, 2012.
- [45] Alimuddin A.M.M. Farea , Shalendra Kumar, Khalid Mujasam Batoo ,Ali Yousef , Chan Gyu Lee, Structure and electrical properties of $\text{Co}_{0.5}\text{Cd}_x\text{Fe}_{2.5-x}\text{O}_4$ ferrites, Journal of Alloys and Compounds Vol.464,pp 361-369, Oct 2007.
- [46] S.A. Mazen, H.M. Zaki and S.F. Mansour, "Infrared Absorption and Dielectric Properties of Mg-Zn Ferrite"International Journal of Pure and Applied Physics (ISSN 0973-177), Issue 1,Vol. 3, pp 40-48, 2007.
- [47] S. S. Shinde, K. M. Jadhav, "Electrical and dielectric properties of silicon substituted cobalt ferrites", Mat. Let., Issue 1-2, Vol. 37, pp 63-67, 1998.
- [48] C. G. koops, "On the dispersion of resistivity and dielectric constant of some semiconductors at audio frequencies", Phys Rev" Vol. 83, pp 121-124,.July 1951..
- [49] A. A. Sattar and Samy A. Rahman, " Dielectric properties of rare earth substituted Cu Zn ferrites", Physica. Status. Solidi (a), Issue 2, Vol. 200, pp 415 –422, Dec. 2003.
- [50] S. A. Rahman, "Temperature, Frequency and Composition Dependence of Dielectric Properties of Nb Substituted Li-ferrites", Egypt. J. Solids, Vol. (29), No. (1),pp 131-140, (2006).